NRC·CNRC

NRC Publications Archive
Archives des publications du CNRC

Understanding particle-particle interactions in cold spraying different sizes of mixed Fe/316L powders from deposition efficiency

Chu, Xin; Che, Hanqing; Teng, Chaoyi; Vo, Phuong; Yue, Stephen

This publication could be one of several versions: author's original, accepted manuscript or the publisher's version. / La version de cette publication peut être l'une des suivantes : la version prépublication de l'auteur, la version acceptée du manuscrit ou la version de l'éditeur.
For the publisher's version, please access the DOI link below./ Pour consulter la version de l'éditeur, utilisez le lien DOI ci-dessous.

Publisher's version / Version de l'éditeur:
https://doi.org/10.1007/s11666-019-00976-9
Journal of Thermal Spray Technology, 29, 3, pp. 413-422, 2019-12-07

NRC Publications Archive Record / Notice des Archives des publications du CNRC :
https://nrc-publications.canada.ca/eng/view/object/?id=2f684813-1b16-44b3-a6d4-b8abff2bb27d
https://publications-cnrc.canada.ca/fra/voir/objet/?id=2f684813-1b16-44b3-a6d4-b8abff2bb27d

Access and use of this website and the material on it are subject to the Terms and Conditions set forth at
https://nrc-publications.canada.ca/eng/copyright
READ THESE TERMS AND CONDITIONS CAREFULLY BEFORE USING THIS WEBSITE.

L'accès à ce site Web et l'utilisation de son contenu sont assujettis aux conditions présentées dans le site
https://publications-cnrc.canada.ca/fra/droits
LISEZ CES CONDITIONS ATTENTIVEMENT AVANT D'UTILISER CE SITE WEB.

Questions? Contact the NRC Publications Archive team at PublicationsArchive-ArchivesPublications@nrc-cnrc.gc.ca. If you wish to email the authors directly, please see the first page of the publication for their contact information.

Vous avez des questions? Nous pouvons vous aider. Pour communiquer directement avec un auteur, consultez la première page de la revue dans laquelle son article a été publié afin de trouver ses coordonnées. Si vous n'arrivez pas à les repérer, communiquez avec nous à PublicationsArchive-ArchivesPublications@nrc-cnrc.gc.ca.

National Research Council Canada | Conseil national de recherches Canada

Canada

Understanding Particle-Particle Interactions in Cold Spraying Different Sizes of Mixed Fe/316L Powders from Deposition Efficiency

Xin Chu [a], Hanqing Che [a] *, Chaoyi Teng [a], Phuong Vo [b], and Stephen Yue [a]

[a] *Department of Mining and Materials Engineering, McGill University, Montreal, Quebec H3A 0C5, Canada*

[b] *National Research Council of Canada, Boucherville, Quebec J4B 6Y4, Canada*

*Corresponding author: Hanqing Che

Email: hanqing.che@mail.mcgill.ca

Tel: +1 514.778.5754

Present address: 2400-3610 University, Montreal, Quebec, H3A 0C5, Canada

Abstract:

In this study, two sizes of Fe and 316L powders are used as the feedstock and they were also premixed using three fractions of the former: (i) large into small for either 316L or Fe, (ii) 316L into Fe using three size combinations. Both single component and mixed Fe/316L powders were deposited by cold spray and DEs (and partial DEs for mixed powders) were calculated and are discussed. Results show that mixing same specie larger powder into the smaller results in a mixture DE following the Rule of Mixtures. Whereas, mixing 316L into Fe generates different DE variations in different size combinations; specifically, smaller size mixtures show improved DEs than the respective single component Fe. The difference in DEs of different sizes of Fe/316L mixtures is explained by particle-particle interactions (i.e. tamping and retention) upon impact. Besides, a relationship between the average particle size and density is generated for the first time to determine the occurrence of particle-particle interactions in cold spray of generic mixed powders. The industrial significance of the knowledge of particle-particle interactions is also explained in fabrications of metal matrix composites (MMCs).

Keywords: Cold spray; Deposition efficiency; Different sizes; Particle-particle interactions; Tamping; Retention

1. Introduction

Cold spray is a relatively new coating technique in which micron-sized (e.g. 10-50 μm) particles are accelerated to supersonic velocities by a high-pressure gas stream in a de-Laval nozzle and are impacted onto substrates in the solid state [1]. Due to its advantages, such as the low process temperature, cold spray has become an effective alternative to fabricate coatings from metals that are highly sensitive to temperature or oxidation [2-4]. During cold spray, not all particles impacting onto substrates necessarily deposit; the term "cold sprayability" is introduced to evaluate the ease with which a powder can be deposited [5]. Deposition efficiency (DE) is one important metric of cold sprayability and is usually defined as the ratio of powder mass deposited to total powder mass sprayed over the substrate [5]. The DE of a powder depends on its material (e.g. hardness, oxide layer thickness) and characteristics (e.g. size, morphology), and can be improved by increasing the "intensity" of cold spray process parameters (i.e. gas pressure and temperature) [6]. In cold spray literature, it has also been reported that adding a second component (SC) powder (ceramic or metal) into a metal can improve its DE [7-9]. This finding is of industrial significance and several examples are: i) to enhance feedstock deposition and adhesion in low-pressure cold spray repair practices (e.g. add Al_2O_3 to various metals [7]); ii) to improve the DE of hard to deposit metals (e.g. add Cu or Zn to Sn [8]) or expensive metals (e.g. add softer or irregular Ta to harder Ta [9]). However, fundamental mechanisms behind such DE improvements in cold spray are often not clear.

To fully understand DE-improving effects, knowledge of interaction behaviors between mixed powders during deposition is required. Regarding the effect that SC applies to matrix powders (SC on matrix), tamping (or hammering, peening) is the one most accepted since SC powders are often large/dense/hard metals or ceramics [8, 10,

11]. Tamping could lead to forced deformation thus further densification of previously deposited layers [11], but its effect on DE is still not clear. For instance, Fernandez et al. [12] proposed that tamping could benefit particle deposition if subsequent hard particles interact with depositing soft particles to enhance interfacial strain and temperature in real time (scenario I in Fig. 1); however, there are still debates over the occurrence of such interactions in cold spray [12-14]. Besides tamping, other common effects of SC on matrix are surface roughening and/or surface activation (removal of surface oxides) which often associate with irregular powder additions (metals [8, 9] or ceramics [11]). Regarding the effect that a matrix applies to SC (matrix on SC), soft/rough deposits could provide a mechanical anchorage effect (e.g. embedding [15] or trapping [8]) to facilitate SC deposition. This explains a certain retention of SC content which cannot reach any deposition alone (e.g. ceramics) in metal/ceramic mixed coatings. Moreover, a few researchers [16, 17] proposed that SC retention can also be contributed by particle-particle interactions: subsequent particles collide with and retain rebounded SC particles (scenario II in Fig. 1). But it is also argued that interactions of excessive/large rebounding particles could otherwise decelerate/deflect subsequent particles to result in reduced DE and defective coatings [10, 18].

In our previous studies, an increase in DE was observed when 316L stainless steel powder was premixed with commercial purity Fe to cold spray fabricate bio-degradable composite stents [19]. To better understand mechanisms of such an improvement, more detailed research towards DE was performed. In this study, DE characteristics of large/small mixtures of 316L or Fe powders, as well as different sizes of binary Fe/316L mixtures were measured and are discussed, and DE-improving mechanisms of mixed Fe/316L mixtures are elucidated. It is proposed that this research finding generates additional insights into documented mechanisms of particle-particle

interactions and provides industrial guidances in cold spray of generic hard/soft mixtures.

2. Materials and Methods

Commercially available gas atomized 316L stainless steel powder (Sandvik Osprey, Neath-Port Talbot, UK) and water atomized commercial purity Fe powder (Goodfellow, Cambridge, UK) are used as the feedstock. Sieving was performed on some powders using 400-mesh (38 μm) sieves to obtain desired particle size distributions and four powders were prepared, namely, Fe large, Fe small, 316L large, and 316L small. SEM images and characteristics of the feedstock are presented in Fig. 2 and Table 1, respectively. The Vickers hardness of the feedstock was measured using a Clark CM-100AT Microhardness Tester (Sun-Tec, Novi, USA) using a load of 10 g and a time of 15 s. The feedstock particle size was determined using a Horiba LA-920 laser diffraction analyzer (Tokyo, Japan). Results show no significant hardness difference between large and small powders of the same material, and spherical 316L has roughly tripled hardness than rounded Fe.

All cold spray campaigns were carried out at the McGill-NRC cold spray facility, located at National Research Council of Canada, Boucherville, using a CGT KINETIKS® 4000 cold spray system (Sulzer Metco, Westbury, USA) with a MOC 24 carbide nozzle. Al 6061 plates with dimensions of 3 × 3 inch (75 × 75 mm) were used as substrates and were blasted with 60 grit alumina to remove scale and promote adhesion. Nitrogen was used as the propellant gas. To investigate effects of mixing powders on DE, aforementioned single component powders were premixed in a rolling mixer (without media) for 1 hour using: (i) 10, 20, 50 wt.% of large into small for either

316L or Fe, and (ii) 10, 20, 50 wt.% of 316L into Fe (10SS, 20SS, 50SS) using three size combinations (Fe small/316L large, Fe large/316L large, Fe small/316L small). The cold spray process parameters were all set at a gas temperature of 600 °C, a gas pressure of 3 MPa, a stand-off distance of 80 mm, a gun travel speed of 300 mm/s, and a feed rate of 20-60 g/min.

After spray, coating cross-sections were characterized using a Hitachi SU3500 SEM (Tokyo, Japan) and composite coating compositions (area fractions of Fe and 316L powders) were estimated by image analyses using a minimum of 30 random images at 200 × magnification. The coating flattening ratio (FR) was calculated as the width to height ratio of a deformed particle from etched cross-sectional optical images at 200 × magnification and the average value was reported about 50 particles per component per sample. The standard error of four average flattening ratio values was also calculated. The particle in-flight velocity was measured in a free jet by an optical time-of-flight particle diagnostic system DPV-2000 (Tecnar Automation, St. Bruno, Canada) under the same process parameters as coating deposition. Velocities of 5000 particles were measured and the average value and standard deviation were calculated for each powder. The DE was measured according to Eq. (1) as mass gain of the substrate divided by total mass of the spray material fed over the substrate. 2-3 measurements were used for each powder composition (relative DE difference < 5 % was obtained) and the average value was reported. In addition to mixture DE, partial DEs (i.e. DEs of the 316L and Fe components in composite coatings) of mixed Fe/316L powders were also calculated based on mixture DE and compositional yield (powder composition vs coating composition) [11, 12].

$$DE = \frac{\Delta m_s \cdot t \cdot v}{\Delta m_f \cdot d} \qquad \text{Eq. (1)}$$

Where, Δm_s is mass change of the substrate after deposition, t is total spray time, v is gun travel speed, Δm_f is mass change of the powder in the hopper after deposition, d is total distance traveled by the nozzle over substrate. The feed rate was calculated as $FR = \frac{\Delta m_f}{t}$.

3. Results

3.1 Mixed particle sizes

The measured in-flight velocities of four single component powders are shown in Table 2. Small powders of either 316L or Fe both have a slightly higher average velocity compared with respective large ones. The large standard deviation of particle velocity is due to the size distribution of each powder.

The DEs of four single component 316L and Fe powders as well as their large/small mixtures are presented in Fig. 3. In each figure, 0 wt.% composition corresponds to only small powder and 100 wt.% composition corresponds to only large powder. Results show that 316L small has doubled DE compared with 316L large (60 % vs 30 %) which is consistent with its slightly higher particle velocity. Whereas, Fe small has similar or even slightly lower DE than Fe large (57 % vs 65 %) despite its higher particle velocity. Moreover, larger powders were added into respective smaller ones and mixture DEs were measured and are plotted in Fig. 3. The predicted mixture DEs calculated by Rule of Mixtures ($DE_{Mix} = DE_{316L} \times f_{316L} + DE_{Fe} \times f_{Fe}$) from non-mixed large and small powders are also plotted as dashed lines. Results show that measured mixture DEs are consistent with predicted values, this indicates inducing large/small particle impacts in cold spray cannot further stimulate DE.

3.2 Mixed Fe/316L powders

The 50SS cross-sectional microstructure of different sizes of Fe/316L composite coatings is shown in Fig. 4. In these images, light regions are 316L, dark regions are Fe, and black spots are pores. In general, all composite coatings are dense, and both Fe and 316L powders in each coating have deformed and are homogenously distributed. It is also noted that 316L powders in deposited coatings are mostly separated by Fe and there is limited 316L-316L contact. The composite coating compositions measured by image analyses are presented in Table 3. In general, the 316L content in each binary Fe/316L composite coating is similar and is always much lower than their initial as-mixed ratios.

The Fe flattening ratios (FR) in single component coatings and different sizes of 50SS coatings were calculated and are presented in Table 4. Note that average FR is commonly used as an indication of the bulk deformation of a spherical particle during deposition [5, 11] thus the value might not be representative of the actual degree of Fe particle deformation due to its rounded morphology. Attention is mainly focused on the relative difference in Fe FR between each coating. Results show that the Fe in different sizes of mixed coatings always exhibits higher flattening ratios compared with respective single component Fe, indicating that a tamping effect of 316L is realized in all mixed coatings. Specifically, the Fe small/316L large combination is observed to be most effective in further deforming Fe compared to Fe small/316L small and Fe large/316L large and exhibits the largest increment of Fe flattening ratios relative to single component Fe (5.3 vs 3.2).

The DE results of single component Fe and 316L powders, as well as different sizes of Fe/316L mixtures are shown in Fig. 5. Regarding mixture DEs (solid lines), results from different sizes of Fe/316L mixtures generally exhibit a decreasing trend with increasing feedstock SS wt.%. This observation is consistent with previous works [20, 21] and it is mainly explained by more presence of poorly deposited 316L on Fe impacts. Moreover, comparing low SS mixtures (10SS and 20SS) with single component Fe in each figure, it is found that additions of 316L in Fe do not necessarily lead to an increase in DE. The DE improvements are observed to be dependent on mixture particle sizes and are only in Fe small/316L large and Fe small/316L small; in particular, a more long-lasting effect (slower rate of DE decrease) is in the latter.

The partial DEs of Fe and 316L components in different sizes Fe/316L mixtures were calculated to understand mixture DEs and results are also plotted in Fig. 5 (dashed lines). In general, variations of partial DEs Fe and 316L in each binary Fe/316L mixture are complicated and they do not necessarily follow same trend with its respective mixture DE. The partial DEs from representative mixtures were compared to investigate the effects of the particle size.

Regarding partial DEs Fe (dashed lines with squares), mixtures of Fe large/316L large (Fig. 5 (b)) and Fe small/316L small (Fig. 5 (c)) were compared. With increasing SS wt.%, the partial DE Fe in Fe large/316L large (line ④) remains relatively unchanged and is the same as the single component Fe DE in left axis; while in Fe small/316L small the partial Fe DE (line ⑤) exhibits a monotonic increase trend and is always higher than its relative single component Fe DE.

Regarding partial DEs 316L (dashed lines with triangles), mixtures of Fe small/316L large (Fig. 5 (a)) and Fe large/316L large (Fig. 5 (b)) were compared. In 10

wt.% SS, the partial DE 316L of Fe small/316L large (line ①) is about 8 % higher than that of Fe large/316L large (line ③). With further increases in feedstock SS wt.%, the former experiences a sudden drop and becomes the same as that of Fe large/316L large, which remains unchanged throughout from 10 to 50 wt.% SS. It is also noticed that there is a similar drop of the partial DE Fe (line ②) along with partial DE 316L (line ①) from 10 to 20 wt.% SS in Fe small/316L large. To sum, above results show that there are significant effects of the particle size on both mixture DEs and partial DEs of mixed Fe/316L powders, which will be discussed in Section 4.

4. Discussion

In the cold spray literature, the effectiveness of tamping is often associated with impact energy and hardness of second component powders [22]. Larger particles can provide more intensive tamping effects than smaller ones due to the higher mass and thus impact energy of an individual particle [23]. In this study, 10, 20, 50 wt.% of larger powders were mixed into respective smaller ones and mixture DEs were measured to be equivalent to predicted DEs calculated based on Rule of Mixtures ($DE_{Mix} = DE_{316L} \times f_{316L} + DE_{Fe} \times f_{Fe}$) (Fig. 3). This observation shows that by simply inducing tamping provided by larger powders of the same specie (i.e. large/small impacts) cannot further stimulate DE in cold spray. It appears that additions of harder powders are necessary to improve DE as observed in Fig. 5 by adding 316L into Fe. To understand mechanisms of DE-improving effects, one possible explanation is associated with fragmentations of Fe surface oxides due to tamping of hard 316L additions which benefits subsequent Fe particles deposition [12, 24]. Following this hypothesis, increasing hard 316L fractions in initial feedstocks would increase tamping

intensity; thus more Fe deposition (i.e. higher partial DE Fe) should be expected. Also, since surface oxide fragmentations are often due to deformation/flattening of particles [24], Fe small/316L large which exhibits largest increment in Fe flattening ratio (Table 4) should exhibit the most significant DE-improving effects compared with the other two combinations. However, measured results in Fig. 5 show that improved DEs are particle-size-dependent and Fe small/316L small instead exhibits the most significant DE-improving effects. Therefore, it is considered that oxide fragmentations induced by impacts of hard 316L additions are not likely to be the main mechanism to explain DE characteristics in different sizes of Fe/316L mixed powders.

As discussed in Section 1, one effective scenario to improve matrix powders deposition through additions of hard powders is that hard particles interact with depositing soft particles to increase their interfacial deformation and contact temperature in real time [12]. In other words, if particle deposition is realized, then the tamping effect of subsequent particles would no longer benefit its deposition (although still increases its deformation) and might otherwise erode it to reduce DE. From this viewpoint, a close inter-particle distance during flight or a short time interval between successive particle impacts is important. Compared with large size feedstocks, using small feedstocks in cold spray could significantly increase particle number density (ND) (ND ~ particle size $(D)^{-3}$) upon impact and potentially establish more SS/Fe interactions. This could explain observations in Fig. 5 that DE-improving effects only occur in smaller size mixtures, i.e. 10 wt.% SS of Fe small/316L large (line ②) and Fe small/316L small (line ⑤).

Similarly, differences in partial DE 316L between each binary Fe/316L mixture can also be explained from particle-particle interactions. In 50SS mixtures with the highest feedstock 316L fractions, 316L particles in deposited coatings are mostly

separated by Fe and there is limited direct 316L-316L contact (Fig. 4). Thus, in all mixing compositions used (10SS, 20SS, 50SS), deposition of a single 316L particle should be only associated with 316L on Fe (impacts) and possible Fe on 316L (interactions). Comparing partial DEs 316L in Fe small/316L large (line ①) and Fe large/316L large (line ③) in Fig. 5, identical and unchanged partial DE 316L is observed from 20 to 50 wt.% SS, this indicates 316L particles in two mixtures experienced the same scenario during deposition. Whereas, in 10 wt.% SS, partial DE 316L in Fe small/316L large (line ①) is ~8 % higher than in Fe large/316L large (line ③); this difference appears to be only explained from the perspective of Fe on 316L, i.e. particle-particle interactions. According to [16], in order to retain a rebounded 316L, its rebound momentum should be overcome by subsequent incoming Fe particles, as shown in Eq. (2).

$$n_{Fe} m_{Fe} v_{Fe} \geq m_r v_r \qquad \text{Eq. (2)}$$

Where, n_{Fe}, m_{Fe}, v_{Fe} are number, mass, and velocity of a subsequent incoming Fe particle, respectively. m_r and v_r are mass and velocity of a rebounded 316L particle. On the right side of Eq. (2), normally, rebound velocity (v_r) of a 316L particle is much lower than its impact velocity [20] due to plastic deformation and adhesive interactions upon impact and retention of a rebounded 316L particle is reasonable. On the left side of Eq. (2), for a given powder feed rate and feedstock mixing fraction, $n_{Fe} m_{Fe}$ is constant. Compared with larger Fe, a smaller Fe mixture not only acquires a higher impact velocity (v_{Fe}) but also a much higher particle number density upon impact, which significantly enhances the probability of a particle hitting another above the substrate. This could explain ~8 % higher DE 316L in Fe small/316L large compared with Fe large/316L large in 10 wt.% SS (Fig. 5). Moreover, in Fig. 5 (a), a similar

decrease of partial DE Fe (line ②) is observed along with partial DE 316L (line ①) from 10 to 20 wt.% SS; this indicates that effects of tamping and retention occur simultaneously upon impact.

From above discussions, it can be concluded that feedstock particle size affects the occurrence of particle-particle interactions, and an improved DE of Fe/316L powders is a result of SS/Fe interactions, i.e. tamping and retention which occur simultaneously during deposition. The simplified schematics of particle-particle interactions in different sizes of low SS mixed Fe/316L powders are presented in Fig. 6. Note that total volume of particles impacting on the substrate in three figures is kept the same. However, due to smaller particle size in Fe small/316L large and Fe small/316L small, a much higher particle number density is realized, leading to SS/Fe particle interactions (i.e. tamping and retention) and improved DEs relative to single component Fe. In particular, Fe small/316L small exhibits the most SS/Fe interactions, therefore most significant DE-improving effects are obtained (Fig. 5 (c)). In Fe small/316L large with increases in feedstock SS wt.%, the large 316L particles replace small Fe which decreases the overall particle number density. This could explain plateaus of partial DE 316L and Fe observed from 20 to 50 wt.% SS (Fig. 5 (a)), indicating no interactions to occur. In Fe large/316L large, due to the low particle number density, it is considered that all particles deposit as an isolated scenario without particle-particle interactions. With increases in feedstock SS wt.%, more poorly deposited 316L on Fe impacts [20, 21] present and its mixture DE monotonically reduces (Fig. 5 (b)).

Besides the particle size, there are also some considerations of the effects of process parameters on particle-particle interactions. A few process parameters were adjusted based on speculations to enhance particle-particle interactions by increasing

particle number density above the substrate (increased feed rate and reduced gun travel speed) or reducing inter-particle in-flight separations (reduced gas temperature/pressure). However, no obvious effects on numbers of particle-particle interactions can be identified (results shown in supplementary file). Thus, feedstock particle size remains the most crucial factor to affect particle number density upon impact and particle-particle interactions above the substrate in cold spray. Based on above findings, the correlations of particle number density (ND) upon impact with regards to powder characteristics and process details can be roughly denoted as:

$$ND \sim \frac{1}{\rho \cdot D^3 \cdot L^2} \qquad \text{Eq. (3)}$$

Where ρ is density of a powder material, D is diameter (size) of a powder, and L is nozzle exit diameter of a specific gun. Using Eq. (3) and critical size of particle-particle interactions in SS/Fe mixtures used in this study (8 g/cm^3, 30 μm), a relationship between the average particle size and density can be plotted to divide the occurrence of particle-particle interactions in cold spray of generic powders, as shown in Fig. 7. The powder characteristics from literature [13, 14, 16, 18] are also plotted for validations and the divisions of particle-particle interactions using this curve are all consistent with the respective researchers' opinions. Note that to the best of our knowledge, the nozzle exit diameters of cold spray guns used in above literature are very close to the one used in this study. This figure thus explains why in literature researchers have different opinions towards the occurrence of particle-particle interactions in cold spray.

These findings of particle-particle interactions could be industrially significant. One example is during fabrications of metal matrix composites (MMCs) when ductile metal powders are premixed with SC powders (e.g. ceramics or hard metals) for subsequent cold spray. From the considerations of particle-particle interactions, if only

a small SC amount is needed, interactions (tamping) can be beneficial and can be realized using hard SC and smaller size mixtures. Conversely, if a high SC amount is needed to exhibit certain functionalities (e.g. ceramics for wear resistance), excessive rebounding of SC powders during deposition might be detrimental to decelerate/deflect subsequent particles and such interactions could be avoided using relatively large size feedstock mixtures.

5. Conclusions

In this study, two sizes of Fe and 316L powders were used as the feedstock. These powders were also premixed using three fractions (10, 20, 50 wt.%) of the former: (i) large into small for either 316L or Fe, (ii) 316L into Fe using three sizes combinations. Both single component and mixed powders were cold spray deposited and deposition efficiency (DE) is mainly studied. The main conclusions can be drawn as follows:

- Adding large powders into respective small ones for either 316L or Fe results in a mixture DE following the Rule of Mixtures ($DE_{Mix} = DE_{316L} \times f_{316L} + DE_{Fe} \times f_{Fe}$); whereas adding hard 316L powders into soft Fe can further improve DE due to SS/Fe particle interactions (i.e. tamping and retention).
- The occurrence of particle-particle interactions upon impact is mainly affected by feedstock particle size. Small SS/Fe mixtures (< 30 μm in this study) exhibit particle-particle interactions due to the high particle number density upon impact.

Acknowledgements

The authors would like to acknowledge the McGill Engineering Doctoral Awards (MEDA) and Natural Sciences and Engineering Research Council of Canada (NSERC) for the financial support. The authors would also like to thank Ms. Caroline Hoang and Mr. Frédéric Belval from National Research Council of Canada, Boucherville for the technical assistance in feedstock preparations, cold spray experiments, and deposition efficiency measurements.

References

[1] A. Moridi, S.M. Hassani-Gangaraj, M. Guagliano, M. Dao, Cold Spray Coating: Review of Material Systems and Future Perspectives, Surf. Eng., 2014, **30**(6), p 369-395

[2] T. Novoselova, P. Fox, R. Morgan, W. O'Neill, Experimental Study of Titanium/Aluminium Deposits Produced by Cold Gas Dynamic Spray, Surf. Coat. Technol., 2006, **200**(8), p 2775-2783

[3] H.Y. Lee, S.H. Jung, S.Y. Lee, K.H. Ko, Alloying of Cold-Sprayed Al–Ni Composite Coatings by Post-Annealing, Appl. Surf. Sci., 2007, **253**(7), p 3496-3502

[4] H.-T. Wang, C.-J. Li, G.-J. Yang, C.-X. Li, Cold Spraying of Fe/Al Powder Mixture: Coating Characteristics and Influence of Heat Treatment on the Phase Structure, Appl. Surf. Sci., 2008, **255**(5), p 2538-2544

[5] W. Wong, P. Vo, E. Irissou, A.N. Ryabinin, J.G. Legoux, S. Yue, Effect of Particle Morphology and Size Distribution on Cold-Sprayed Pure Titanium Coatings, J. Therm. Spray Technol., 2013, **22**(7), p 1140-1153

[6] H. Aydin, M. Alomair, W. Wong, P. Vo, S. Yue, Cold Sprayability of Mixed Commercial Purity Ti plus Ti6Al4V Metal Powders, J. Therm. Spray Technol., 2017, **26**(3), p 360-370

[7] T. Piwowarczyk, M. Winnicki, A. Małachowska, A. Ambroziak, Casting Defects Filling by Low Pressure Cold Spraying Method, Arch. Foundry Eng., 2014, **14**(1), p 109-114

[8] H. Che, X. Chu, P. Vo, S. Yue, Cold Spray of Mixed Metal Powders on Carbon Fibre Reinforced Polymers, Surf. Coat. Technol., 2017, **329**, p 232-243

[9] S. Yue, W. Wong, H. Aydin, R. Mongrain, R. Barua, P. Vo, R. Dolbec, Improving Cold Sprayability: Mixed Metal Powders, *Thermal Spray 2015: Proceedings of the International Thermal Spray Conference*, A. McDonald, A. Agarwal, G. Bolelli, A. Concustell, Y.-C. Lau, F.-L. Toma, E. Turunen, and C. Widener, Ed., May 11-14, 2015 (Long Beach, California), Springer, 2016, 473 p

[10] R.G. Maev, V. Leshchynsky, Air Gas Dynamic Spraying of Powder Mixtures: Theory and Application, J. Therm. Spray Technol., 2016, **15**(2), p 198-205

[11] E. Irissou, J.-G. Legoux, B. Arsenault, C. Moreau, Investigation of Al-Al2O3 Cold Spray Coating Formation and Properties, J. Therm. Spray Technol., 2007, **5**(16), p 661-668

[12] R. Fernandez, B. Jodoin, Cold Spray Aluminum-Alumina Cermet Coatings: Effect of Alumina Content, J. Therm. Spray Technol., 2018, **27**(4), p 603-623

[13] K. Ito, Y. Ichikawa, Microstructure Control of Cold-Sprayed Pure Iron Coatings Formed Using Mechanically Milled Powder, Surf. Coat. Technol., 2019, **357**, p 129-139

[14] J. Perry, P. Richer, B. Jodoin, E. Matte, Pin Fin Array Heat Sinks by Cold Spray Additive Manufacturing: Economics of Powder Recycling, J. Therm. Spray Technol., 2018, **28**(1-2), p 144-160

[15] X.-T. Luo, Y.-K. Wei, Y. Wang, C.-J. Li, Microstructure and Mechanical Property of Ti and Ti6Al4V Prepared by an In-Situ Shot Peening Assisted Cold Spraying, Mater. Des., 2015, **85**, p 527-533

[16] P.C. King, S.H. Zahiri, M.Z. Jahedi, Rare Earth/Metal Composite Formation by Cold Spray, J. Therm. Spray Technol., 2017, **17**(2), p 221-227

[17] S. Ahmad Alidokht, P. Vo, S. Yue, R.R. Chromik, Erosive Wear Behavior of Cold-Sprayed Ni-WC Composite Coating, Wear, 2017, **376**, p 566-577

[18] S.M. Hassani-Gangaraj, A. Moridi, M. Guagliano, Critical Review of Corrosion Protection by Cold Spray Coatings, Surf. Eng., 2015, **31**(11), p 803-815

[19] R. Barua, "Study of the Structural Properties and Control of Degradation Rate for Biodegradable Metallic Stents using Cold Spray," Ph.D. Thesis, McGill University, 2015

[20] X. Chu, R. Chakrabarty, H. Che, L. Shang, P. Vo, J. Song, S. Yue, Investigation of the Feedstock Deposition Behavior in a Cold Sprayed 316L/Fe Composite Coating, Surf. Coat. Technol., 2018, **337**, p 53-62

[21] X. Chu, H. Che, P. Vo, R. Chakrabarty, B. Sun, J. Song, S. Yue, Understanding the Cold Spray Deposition Efficiencies of 316L/Fe Mixed Powders by Performing Splat Tests onto As-Polished Coatings, Surf. Coat. Technol., 2017, **324**, p 353-360

[22] W.Y. Li, C. Zhang, H.T. Wang, X.P. Guo, H.L. Liao, C.J. Li, C. Coddet, Significant Influences of Metal Reactivity and Oxide Films at Particle Surfaces on Coating Microstructure in Cold Spraying, Appl. Surf. Sci., 2017, **253**(7), p 3557-3562

[23] Y.-K. Wei, X.-T. Luo, C.-X. Li, C.-J. Li, Optimization of In-Situ Shot-Peening-Assisted Cold Spraying Parameters for Full Corrosion Protection of Mg Alloy by Fully Dense Al-based Alloy Coating, J. Therm. Spray Technol., 2016, **26**(1-2), p 173-183

[24] X.-T. Luo, M.-L. Yao, N. Ma, M. Takahashi, C.-J. Li, Deposition Behavior, Microstructure and Mechanical Properties of an In-Situ Micro-Forging Assisted Cold Spray Enabled Additively Manufactured Inconel 718 Alloy, Mater. Des., 2018, **155**, p 384-395

Figure captions:

Fig. 1 Schematic diagram of particle-particle interactions (i.e. collisions between moving particles) during mixed powders deposition (summarized from [12, 16]).

Fig. 2 SEM images of the feedstock.

Fig. 3 The DEs of large/small mixtures. (a) Fe small/Fe large and (b) 316L small/316L large. Dashed lines indicate predicted mixture DEs calculated by the Rule of Mixtures ($DE_{Mix} = DE_{316L} \times f_{316L} + DE_{Fe} \times f_{Fe}$).

Fig. 4 The BSE images of 50SS Fe/316L composite coating cross-sections. (a) Fe small/316L large, (b) Fe large/316L large, and (c) Fe small/316L small.

Fig. 5 The DE and partial DE results of different sizes of Fe/316L mixtures. (a) Fe small/316L large, (b) Fe large/316L large, and (c) Fe small/316L small.

Fig. 6 Simplified schematics of particle-particle interactions in different sizes of low SS mixed Fe/316L powders. (a) Fe small/316L large, (b) Fe large/316L large, and (c) Fe small/316L small.

Fig. 7 Divisions of particle-particle interactions using Eq. 3 and critical size of SS/Fe mixtures and powder characteristics plots from other literature (+: interactions; −: no interactions).

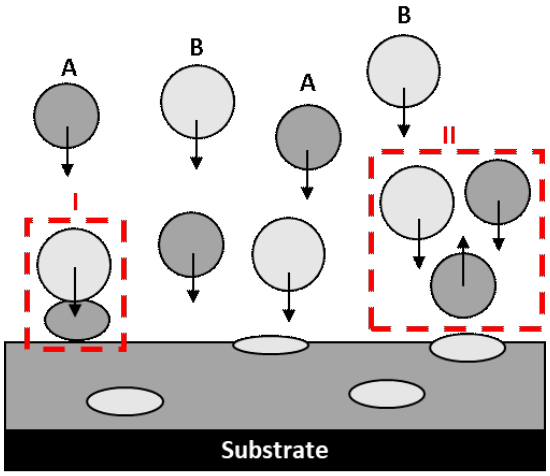

Fig. 1 (color online)

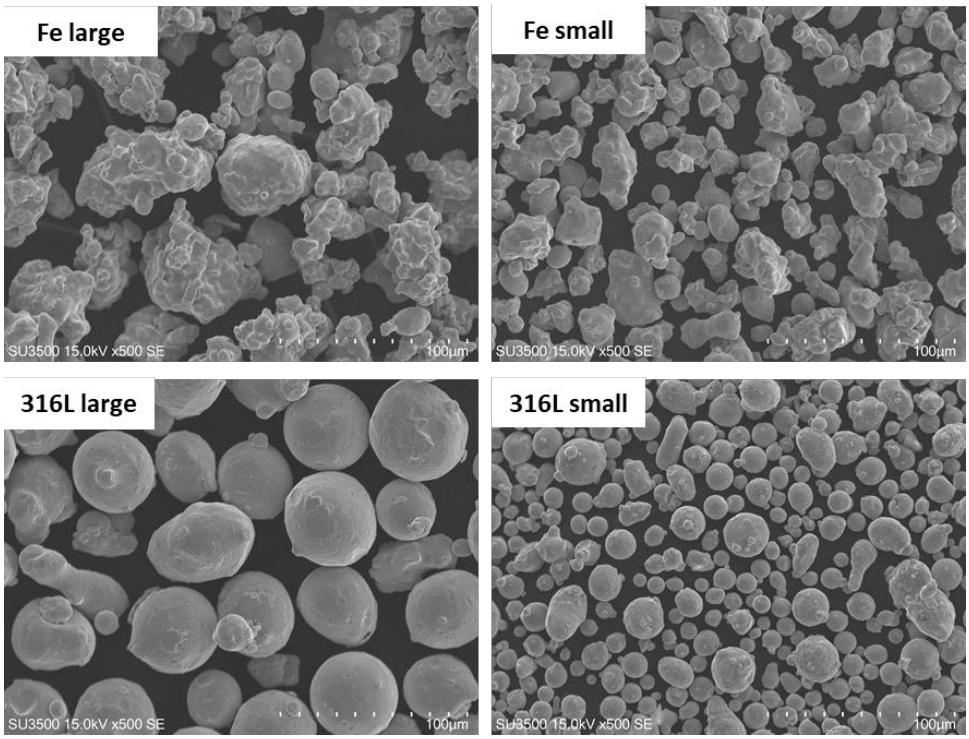

Fig. 2

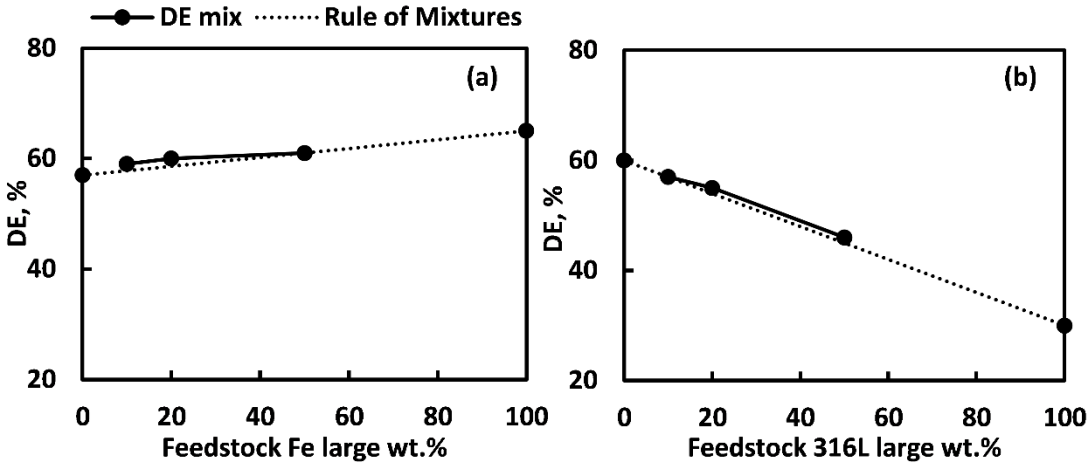
DE mix
Rule of Mixtures
(a)
(b)
DE, %
80
60
40
20
0
20
40
60
80
100
Feedstock Fe large wt.%
Feedstock 316L large wt.%

Fig. 3

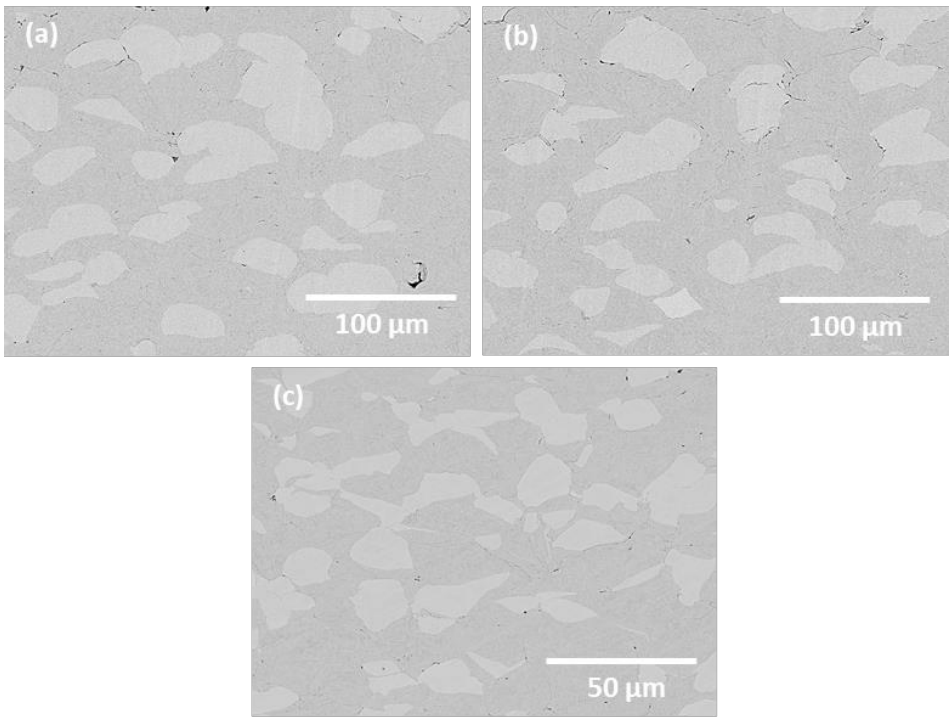
(a)
100 µm
(b)
100 µm
(c)
50 µm

Fig. 4

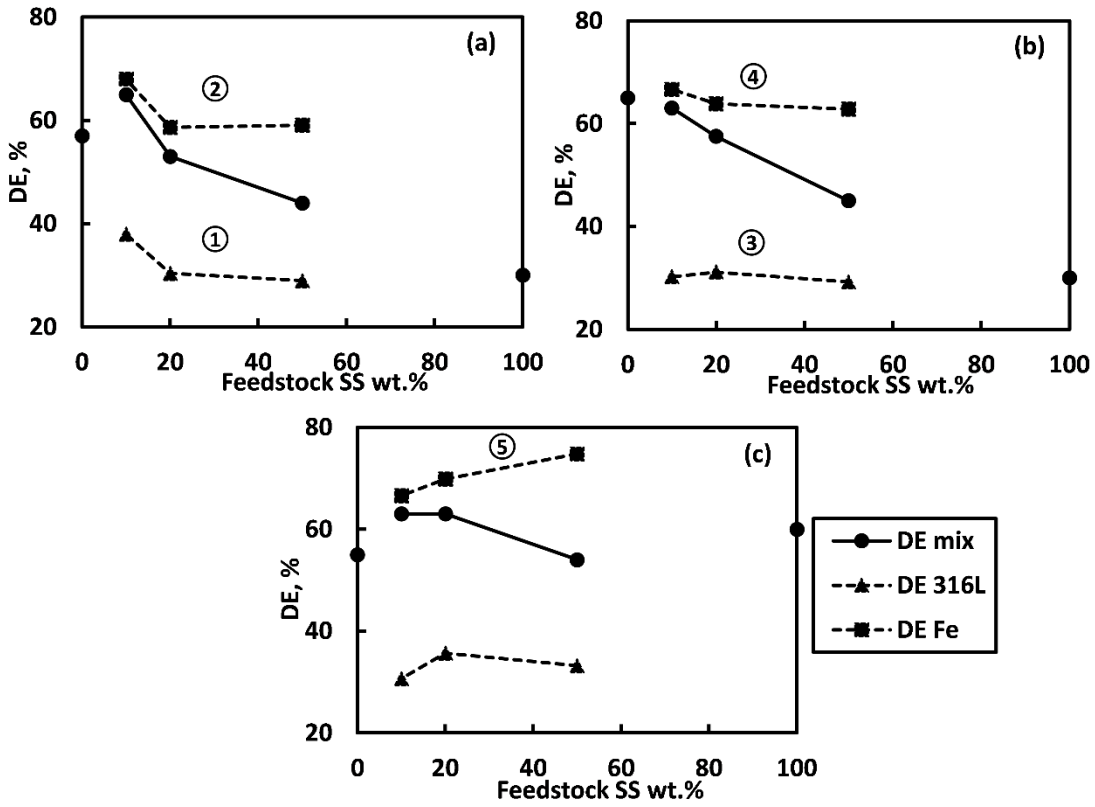

Fig. 5

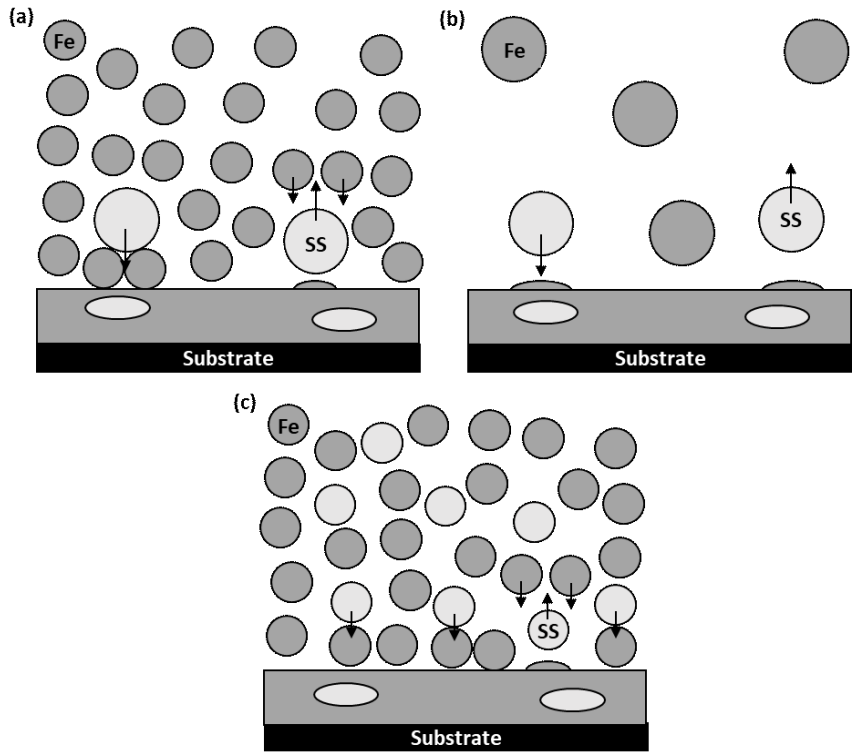

Fig. 6

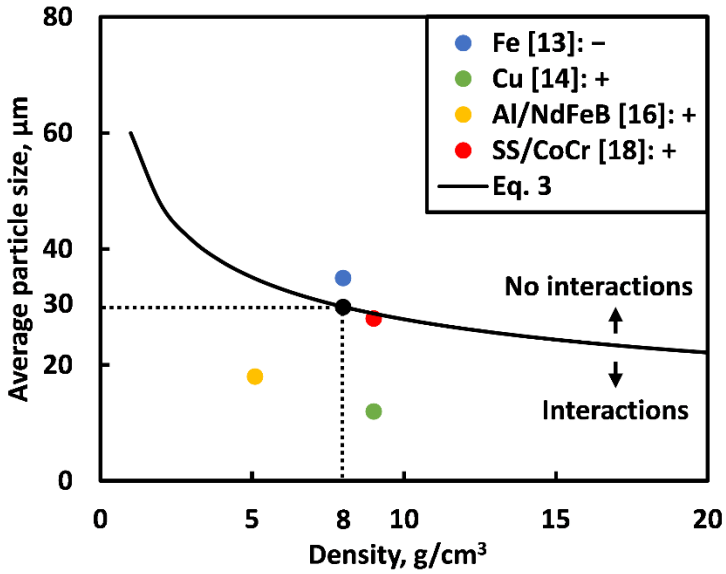

Fig. 7 (color online)

Table 1 Characteristics of the feedstock.

Feedstock	Microhardness, $HV_{0.01}$	d10, µm	d50, µm	d90, µm
Fe large	127 ± 19	29.5	46.7	67.8
Fe small	118 ± 15	17.6	27.8	43.2
316L large	353 ± 11	36.7	46.1	57.7
316L small	347 ± 13	11.7	17.7	25.5

Table 2 The measured in-flight velocities of single component powders.

Feedstock	Particle velocity, m/s
Fe small	612 ± 107
Fe large	584 ± 67
316L small	583 ± 112
316L large	552 ± 70

Table 3 The average 316L weight fractions in different sizes of Fe/316L composite coatings.

Coating	Fe small/316L large	Fe large/316L large	Fe small/316L small
10SS	5.8 ± 0.2	4.8 ± 0.6	4.9 ± 0.5
20SS	11.5 ± 0.4	11.2 ± 0.5	11.3 ± 0.5
50SS	32.9 ± 1.3	30.2 ± 0.7	30.7 ± 0.7

Table 4 The Fe flattening ratios in single component and 50SS mixed Fe/316L coatings.

Coating	Fe flattening ratio
Fe small	3.2 ± 0.1
Fe large	3.4 ± 0.2
Fe small/316L large	5.3 ± 0.2
Fe large/316L large	3.7 ± 0.1
Fe small/316L small	3.6 ± 0.3